Wigner distribution function for finite systems

Natig M. Atakishiyev,[a),b)] Sergey M. Chumakov, and Kurt Bernardo Wolf
Instituto de Investigaciones en Matemáticas Aplicadas y en Sistemas—Cuernavaca, Universidad Nacional Autónoma de México, Apartado Postal 48-3, 62251 Cuernavaca, Morelos, México

(Received 9 May 1997; accepted for publication 11 August 1998)

We construct a Wigner distribution function for finite data sets. It is based on a finite optical system; a linear wave guide where the finite number of discrete sensors is equal to the number of modes which the guide can carry. The dynamical group for this model is SU(2) and the wave functions are sets of $N=2l+1$ data points. The Wigner distribution function assigns classical *c*-numbers to the operators of position, momentum, and wave guide mode. © *1998 American Institute of Physics.* [S0022-2488(98)00312-0]

I. CONTINUOUS AND FINITE SIGNAL ANALYSIS

The phase-space representation of data sets can be analyzed with the aid of the Wigner distribution function. This was introduced originally in quantum mechanics, where the ''signal'' is a wave function $\psi(q)$, and its Wigner function (for $\hbar=1$) is defined as[1]

$$W_\psi(q,p)=\frac{1}{2\pi}\int_{\mathfrak{R}} dx[\,\psi(q-\tfrac{1}{2}x)]^* e^{-ixp}\psi(q+\tfrac{1}{2}x). \tag{1.1}$$

When (q,p) are understood as canonically conjugate coordinates of a phase-space plane, the value of $W_\psi(q,p)$ mirrors closely the intuitive objects in the model. They can be ''particles'' in quantum mechanics, with position q and canonically conjugate momentum p; in quantum optics these objects may be the coherent states of the radiation field; in monochromatic paraxial wave optics they are often beams with Gaussian position and inclination distributions. The Heisenberg uncertainty relation is built into the Wigner picture by the Fourier transform between the position and momentum representations.

The importance of the Wigner distribution function on finite data sets can be explained in terms of Lohmann's rendering of the Wigner function in music,[2] whereas the graphs of the acoustic signal or the frequency spectrum of a performance are meaningless to visual inspection, the Wigner function will exhibit peaks at positions that are the notes in a pentagram. In effect, the Wigner function is a musical score—*partitura* of the data set $\{\psi(q)\}$, $q\in\mathfrak{R}$, which also contains the information of its Fourier transform function $\{\tilde{\psi}(p)\}$, $p\in\mathfrak{R}$. Lohmann also presents optical devices to produce essentially a photograph of the Wigner function of a line segment of data on a slide.[3]

In this paper we analyze specifically the phase-space representation of finite data sets. We are interested in the features specific to finite systems. They include the discreteness of measurement and operator spectra, and the fact that these operators are realizations of a compact Lie algebra of *difference* operators. Physicists using Lie-theoretical methods are much more familiar with algebras of *differential* operators. We should stress that the domain of difference operators are functions on the complex plane; in the same way as the difference equation $\Gamma(x+1)=x\Gamma(x)$ generalizes the factorial product of the nonnegative integers to any $x\in\mathfrak{R}$, difference operators will generally relate three neighboring points of x separated by unity. Moreover, finite difference equations have a recognizedly richer structure of solutions than their limit differential equations.[4] When the interval and density of data points approach infinity, the results obtained will match with those of the standard formalism for continuous signals.

[a)]Electronic mails: natig@, sergey@, and bwolf@ce.ifisicam.unam.mx
[b)]Instituto de Matemáticas, UNAM, Mexico.

We consider $2l+1$ complex data values

$$\mathbf{f}=\{f_m | m=-l,-l+1,...,l\}, \quad f_m \in \mathcal{C}, \tag{1.2a}$$

where $2l+1$ is a non-negative integer. These can be thought of as complex light amplitude values measured on an array of $2l+1$ points on a screen, equidistant by $\lambda>0$ and centered at the origin, i.e.,

$$f_m=f(q_m), \quad q_m=m\lambda, \quad m=-l,-l+1,...,l. \tag{1.2b}$$

In ordinary finite Fourier analysis one asks for the exponential Fourier transform to provide the wave number content $\tilde{\mathbf{f}}$ of the signal $\mathbf{f}$ in the $2l+1=N$-dimensional orthonormal basis $N^{-1/2}\exp(2\pi mn/N)$, $n=1,...,N$, consisting of Brillouin waves in a periodic lattice. This basis is adequate for a model of a finite system if the system is homogeneous under (dihedral) rotations of the lattice, so the points q_{-l} and q_l are first neighbors. When the two points q_{-l} and q_l are poles apart of an array where the middle portion carries the most significant part of the information, a different basis and transform are called for. Moreover, since the spectrum of the finite second-difference matrix is not equally spaced, the finite Fourier-exponential transform[5] is a poor basis for Lie-theoretical classification and evolution treatment of finite data in a system.

In Sec. II we present the finite wave guide model.[6] This is a physical system which embodies well the mathematical developments we present below; it is a *finite oscillator*. As will become clear at the end of the paper, the wave guide model serves as a working definition of *finite optics*. We start with Newton's equation for the classical harmonic oscillator, and show that both the usual infinite-spectrum quantum mechanical oscillator and the present finite-spectrum oscillator satisfy that equation; the former with the Heisenberg–Weyl algebra, the latter with the su(2) compact algebra. We stress that our approach uses the group of 2×2 unimodular unitary matrices (twofold cover of the rotation group in three dimensions), rather than the usual Heisenberg–Weyl group, as an arena for the Wigner function. In this way, we are assured of the existence of a *position* operator whose spectrum, $m=-l,-l+1,...,l$, is discrete and finite.

Section III defines the Wigner operator in the group ring,[7] and the Wigner distribution function as a bilinear form of the data values, which depend on the classical position, momentum, and energy variables. Section IV examines the SU(2) covariance of the Wigner function and addresses its computation by using group theoretical properties. It is clarified that for each fixed number of sensors $N=2l+1$, the essential information can be plotted and inspected visually on the surface of a two-sphere. Coherent SU(2) states are examined in Sec. V, where we also plot other interesting data sets, such as Schrödinger-cat states with their concomitant interference phenomenon. The concluding Sec. VI recapitulates our construction and indicates other finite systems with various dynamical laws, which can be analyzed by the same mathematical tools and physical concepts.

II. FINITE WAVE GUIDE MODEL AND THE SU(2) GROUP

Finite data sets and their parallel processing by optical means will be based on a planar multimodal wave guide, such as would be part of photonic devices fabricated by doping a strip on a transparent substratum.[6] The *finite* wave guide model has a refractive index whose profile is parabolic (i.e., of the form $n(q)=n_0-\nu q^2+\cdots$ in a neighborhood of its axis); it acts as a harmonic oscillator on the input wave field (signal) produced by a linear array of N coherent light sources; the output is received by the same number of wave field sensors. We stress that our wave guide model is capable of carrying only a *finite* number of modes, and corresponds to a quantum system with finite number of bound states equidistant in energy (see Fig. 1).

A. Newton equation for the finite oscillator

A unit mass in the classical one-dimensional harmonic oscillator potential $V(q)=\frac{1}{2}\omega^2 q^2$ obeys Newton's equation $\ddot{q}=-\omega^2 q$ (the dots indicate time derivatives); the same equation applies in geometric optics to the transverse ray coordinate within a wave guide. As in the quantization (or *wavization*) of geometric to paraxial wave (Fourier) optics,[8] we assume that there exists a *position* operator Q, and time derivatives of the classical observables are replaced by Lie brackets (commutators) of the corresponding operators with a Hamiltonian evolution operator H (times i). For the systems at hand, Newton's equation thereby becomes the *Lie–Newton equation*

$$[H,\,[H,\,Q]]=\omega^2 Q. \tag{2.1a}$$

By definition, the commutator of the Hamiltonian and position operators yields the *momentum* operator

$$P=i[H,\,Q], \tag{2.1b}$$

so the Lie–Newton equation (2.1a) becomes

$$[H,\,P]=i\omega^2 Q. \tag{2.1c}$$

The three operators Q, P, and H satisfy two commutation relations, (2.1b) and (2.1c), which embody the *Hamilton* equations of oscillator/wave guide systems; their geometry and dynamics, respectively. Notice that the third commutator, $[P, Q]$, is so far unspecified; for the three operators to close into a Lie algebra, their Jacobi identity requires that $[H,\,[P,\,Q]]=0$. This implies that $[P, Q]$ is constant under evolution by H, and has the form

$$[P,\,Q]=i(\sigma H+C), \tag{2.2}$$

where $\sigma\in\{+1,0,-1\}$, and C is any operator that commutes with the original three, i.e., is in the center of the Lie algebra. [We placed the i in (2.2) to use self-adjoint operators below.] The values of the coefficient σ determine the *dynamical* Lie algebra to be su(2), iso(2) or su(1,1), respectively, and C may be a function of the Casimir invariant plus/or the generator of a central extension, plus/or a constant. [If a nonlinear function of H is placed in (2.2), other algebraic structures may arise; we will not examine them here.]

In the familiar formulation of quantum phase space with operators Q and P, one sets $\sigma=0$ and $C=\hbar\mathbf{1}$; this defines the Heisenberg–Weyl–Lie algebra, and Eqs. (2.1) are satisfied when $H=\frac{1}{2}(P^2+\omega^2Q^2)$, in accordance with the classical Hamiltonian formulation.[9] In Fourier polychromatic optics, the natural constant $\hbar$ is replaced by the reduced wavelength $\lambda/2\pi$, $\lambda\in\Re-\{0\}$.[7] In Ref. 10 we examined the case when in (2.1a) and (2.1c) the oscillator frequency ω is zero, and in (2.2) $\sigma=-1$, $C=0$; we have then a Euclidean dynamical Lie algebra, iso(2). In this article we shall examine the su(2) structure that fits the finite wave guide model.

B. Difference operators for finite systems

In finite systems, the position coordinate ranges over a finite (discrete) set of integer (or half-integer) values, $q_m=m$, $m=-l,-l+1,...,l$. This set of values we here interpret as the *spectrum* of the position operator Q of the model, in a $(2l+1)$-dimensional vector space $\Re^{2l+1}$ of signals (1.2).

Denoting by $q\in\Re$ the continuous coordinate whose integer (or half-integer) values are the normalized sensor positions m, and using the right- and left-shift operators $e^{\pm\partial_q}f(q)=f(q\pm1)$, we recall from Refs. 6 and 11 the *difference* operators

$$J_1=Q=q, \tag{2.3a}$$

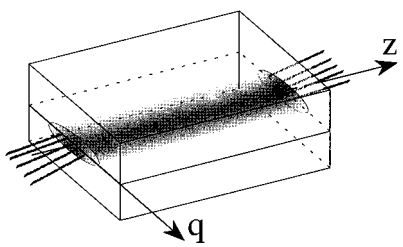

FIG. 1. Finite wave guide model. A shallow, planar wave guide doped into a transparent substrate, capable of confining only $2l+1$ transverse modes, transmits in parallel at most that number of signals to the same number of sensors.

$$J_2 = -P = -i\tfrac{1}{2}[\alpha_l(-q)e^{\partial_q} - \alpha_l(q)e^{-\partial_q}], \quad \alpha_l(q) = \sqrt{(l+q)(l-q+1)}, \tag{2.3b}$$

$$J_3 = H - l - \tfrac{1}{2} = -\tfrac{1}{2}[\alpha_l(q)e^{-\partial_q} + \alpha_l(-q)e^{\partial_q}]. \tag{2.3c}$$

These operators satisfy the Lie–Hamilton commutation relations (2.1) and (2.2) with $\sigma = +1$ and $C = -(l+\frac{1}{2})\mathbf{1}$, as generators of a Lie algebra su(2),

$$[J_1, J_2] = iJ_3, \quad [J_2, J_3] = iJ_1, \quad [J_3, J_1] = iJ_2. \tag{2.4}$$

Since the Casimir operator in this realization is $J^2 = J_1^2 + J_2^2 + J_3^2 = l(l+1)\mathbf{1}$, it is equivalent to the SU(2) unitary irreducible representation familiar from quantum angular momentum theory, but with J_1 identified as the position operator.

In this way the angular momentum algebra su(2) is woven into the foundation of finite systems, i.e., systems with a finite number of independent states, and in particular of the multimodal planar wave guide model. The spectra of positions, momenta, and energies are intrinsically discrete, finite, and equally-spaced. When we change the basis (2.3), so that the Hamiltonian $H = J_3 + l + \frac{1}{2}$ be diagonal, we find the eigenvalue equation

$$H(q)\phi_n(q,2l) = (n+\tfrac{1}{2})\phi_n(q,2l), \quad n = 0,1,...,2l, \tag{2.5}$$

that governs the wave field normal modes in the finite wave guide. The eigenfunctions $\phi_n(q,2l)$ can be written in terms of Kravchuk polynomials,[12] which satisfy a discrete orthogonality relation with a binomial weight function. Multiplying the polynomials with the square root of the latter defines the Kravchuk *functions*,[6,13] which are continuously defined in the interval $-l-1 \leqslant q \leqslant l+1$ and satisfy the discrete orthogonality relation $\Sigma_{m=-1}^{l} \phi_n'(m,2l)\phi_{n'}(m,2l) = \delta_{n,n'}$. In Ref. 13 we showed that when $l \to \infty$ and the spacing between points vanishes as l^{-1}, they become the usual quantum harmonic oscillator wave functions.

C. Polar parametrization of SU(2)

Exponentiation of the Lie algebra of operators (2.3) yields the elements of the SU(2) group, whose generic element can be parametrized by a three-vector $\mathbf{y}$, whose unit direction vector $\mathbf{v} = \mathbf{y}/|\mathbf{y}|$ is the rotation axis, and whose length $\eta = |\mathbf{y}|$ is the rotation angle around that axis, namely,

$$g[\mathbf{y}] = g[\eta\mathbf{v}] = \exp(-i\mathbf{y}\cdot\mathbf{J}) = \exp[-i\eta(v_1J_1 + v_2J_2 + v_3J_3)]. \tag{2.6}$$

$$\mathbf{y} = \eta\mathbf{v}(\theta,\phi), \quad \mathbf{v} = \begin{pmatrix} \sin\theta\sin\phi \\ \sin\theta\cos\phi \\ \cos\theta \end{pmatrix}, \quad \begin{cases} 0 \leqslant \eta < 4\pi, \\ 0 \leqslant \theta \leqslant \pi, \\ 0 \leqslant \phi < 2\pi. \end{cases} \tag{2.7}$$

This is the *polar* parametrization of the group, indicated hereafter by the square brackets; it provides an $\mathfrak{R}^3$ coordinate system where the unit element is at the origin, $g[\mathbf{0}]$, for all directions (θ,ϕ) and the SU(2) ''minus unit,'' also in the center (commutant) of the group, is the element $g[2\pi\mathbf{v}(\theta,\phi)]$, also for all directions. The vanishing of the Haar measure at $\eta = 0,2\pi$ in Eq. (2.10) below, indicates that each of these element counts for a single point of the manifold. In polar coordinates, the nth power is simply expressed as $(g[\mathbf{y}])^n = g[n\mathbf{y}]$; this defines fractional powers and yields the inverse element for $n = -1$. The angle η is counted modulo 4π and labels the conjugation classes of the group; the group elements within each class are distinguished by the axis $\mathbf{v}(\theta,\phi) \in \mathcal{S}_2$ on the two-sphere. (Relations with the more commonly used Euler angle parametrization $g(\phi,\theta,\psi)$ (Refs. 14, 15), indicated by round brackets, will appear below.)

The three generators $\mathbf{J} = (J_1, J_2, J_3)$ transform under the action of the SU(2) group as the components a row vector under the *adjoint* representation $\mathbf{R}$ by 3×3 orthogonal matrices

$$g[\mathbf{z}]\mathbf{J}(g[\mathbf{z}])^{-1} = \mathbf{J}\mathbf{R}[\mathbf{z}]. \tag{2.8}$$

The generic operator in the su(2) algebra has the form $\mathbf{y}\cdot\mathbf{J} = \Sigma_{i=1}^{3} y_i J_i$; therefore, from (2.6) and writing $\mathbf{y} = \eta\mathbf{v}(\theta,\phi)$, it follows that in polar parametrization,

$$g[\mathbf{z}]g[\mathbf{y}](g[\mathbf{z}])^{-1}=g[\mathbf{R}[\mathbf{z}]\mathbf{y}]=g[\,\eta\mathbf{R}[\mathbf{z}]\mathbf{v}]. \tag{2.9}$$

In these coordinates, the invariant measure [for which $\int_{SU(2)} dg\ f(g)=\int_{SU(2)} dg\ f(gg_0)=\int_{SU(2)} dg\ f(g^{-1})$] is[14,15]

$$dg[\mathbf{y}]=\gamma(\eta)d\mathbf{y}=\tfrac{1}{2}\sin^2\tfrac{1}{2}\eta d\,\eta d\mathbf{v},\quad d\mathbf{v}(\vartheta,\varphi)=\sin\vartheta d\vartheta d\varphi, \tag{2.10a}$$

where $d\mathbf{y}=dy_1\,dy_2\,dy_3$ is the Cartesian measure in $\mathfrak{R}^3$, the weight function is

$$\gamma(\eta)=\frac{\frac{1}{2}\sin^2\frac{1}{2}\eta}{\eta^2}=\tfrac{1}{8}\,\mathrm{sinc}\,\tfrac{1}{2}\eta, \tag{2.10b}$$

and $\mathrm{sinc}\,x=x^{-1}\sin x$ is the *sinus cardinalis* function. Finally, we recall that the SU(2) manifold is the three-sphere $\mathcal{S}_3$ and $\mathrm{vol\,SU(2)}=\int_{SU(2)}dg=2\pi^2=\mathrm{vol}\,\mathcal{S}_3$.

On the su(2) algebra, the Hamiltonian generates evolution through $g[z,\mathbf{k}]=\exp(-izH)$, i.e., a rotation by the angle z around the unit vector $\mathbf{k}$ along the three-axis. In the finite wave guide model defined by (2.3), it represents evolution of the $\mathfrak{R}^{2l+1}$ wave fields along the optical z-axis of the wave guide (times a common phase $\exp[-iz(l+\frac{1}{2})]$). Other useful optical elements are also contained in this su(2) model; a thin *wedge* (prism) of distinct refracting index in the wave guide, of small angle ω, multiplies the signal along the sensor array by $e^{-i\omega m}$; this is generated by Q and is a rotation by ω around the one-axis of the group. A tilted plate of such material *translates* signal positions at the center of the guide; it is a rotation around the two-axis of the group generated by P.

III. WIGNER OPERATOR AND DISTRIBUTION FUNCTION

In this section we define the Wigner operator on a Lie group[7] and examine the SU(2) Wigner function associated with the finite wave guide model.

A. Wigner operator and its covariance

Consider a d-parameter Lie group $\mathcal{G}$ with generators $\mathbf{J}=\{J_i\}_{i=1}^d$, whose elements in polar parametrization are $g[\mathbf{y}]=\exp(-i\mathbf{y}\cdot\mathbf{J})$, where $\mathbf{y}\cdot\mathbf{J}:=\Sigma_{j=1}^D y_jJ_j$. We define the *Wigner operator* as the family of formal operators, function of $\mathbf{x}\in\mathfrak{R}^d$, given by

$$\mathcal{W}(\mathbf{x})=\int_{\mathcal{G}}dg[\mathbf{y}]\exp[i\mathbf{y}\cdot(\mathbf{x}-\mathbf{J})]=\int_{\mathcal{G}}dg[\mathbf{y}]\exp(i\mathbf{x}\cdot\mathbf{y})g[\mathbf{y}]. \tag{3.1}$$

In the case of the unitary group SU(2), $d=3$ and the dot product is the rotation-invariant scalar product between three-vectors, $\mathbf{x}\cdot\mathbf{y}=\Sigma_{i=1}^3 x_iy_i$. The direct integral of group elements is well defined when the operator acts on functions over a homogeneous space under the group; the SU(2)-invariant measure is (2.10).

Note first that the Wigner operator at the coordinate origin, $\mathcal{W}(\mathbf{0})=\mathcal{I}$, is the unit element in the SU(2) group ring of formal operators $\mathcal{A}=\int_{\mathcal{G}} dg\ A(g)g$ (i.e., $\mathcal{I}\mathcal{A}=\mathcal{A}\mathcal{I}=\mathcal{A}$). Next, observe that the range of the polar parameters $\mathbf{y}$ is the compact SU(2) manifold, while the space $\mathbf{x}$ in the argument of the Wigner operator is $\mathfrak{R}^3$. Moreover, the function $\exp(i\mathbf{x}\cdot\mathbf{y})$ in (3.1) is not periodic over the group; for general $\mathbf{x}$ it has different values at $g[\,\eta\mathbf{v}]$ and at $g[(\eta+4\pi)\mathbf{v}]$, which represent the same element $g[\mathbf{y}]$. We must therefore fix the definition of the Wigner operator (3.1) by imposing an otherwise natural condition for operators in Lie group rings, self-adjointness. We consider the group elements $g[\mathbf{y}]$ in (3.1) acting as unitary operators on an appropriate Hilbert space, so their operator adjoint is their inverse, $(g[\mathbf{y}])^\dagger=g[-\mathbf{y}]$. Then, we obtain the adjoint of $\mathcal{W}(\mathbf{x})$ through complex conjugation of the exponential function; changing integration variables by $\mathbf{y}\mapsto-\mathbf{y}$, we reproduce (3.1) only if $\int_{SU(2)} dg[-\mathbf{y}]\cdots=\int_{SU(2)} dg[\mathbf{y}]\cdots$. The range of $\mathbf{y}=\eta\mathbf{v}(\theta,\phi)$ will be the same as that of its inverse $-\mathbf{y}$ if we agree that η, naturally ranging in $[0,4\pi)$ in accordance with (2.6)–(2.7) and counted modulo 4π, will be integrated over $(-2\pi,2\pi]$. Only in this way the Wigner operator will be self-adjoint (in the same Hilbert space): $[\mathcal{W}(\mathbf{x})]^\dagger=\mathcal{W}(\mathbf{x})$ for all $\mathbf{x}\in\mathfrak{R}^3$.

The Wigner operator (3.1) satisfies the important property of SU(2)-*covariance*,

$$g[\mathbf{y}]\mathcal{W}(\mathbf{x})(g[\mathbf{y}])^{-1}=\mathcal{W}(\mathbf{R}[\mathbf{y}]\mathbf{x}). \tag{3.2a}$$

This is a consequence of the bilateral invariance of $dg[\mathbf{y}]$ and the property (2.9) of the adjoint representation; it follows from rewriting the left-hand side of (3.2a) as

$$\int_{\mathrm{SU}(2)} dg[\mathbf{y}]\exp(i\mathbf{y}'\cdot\mathbf{x})g[\mathbf{R}\mathbf{y}']=\int_{\mathrm{SU}(2)} dg[\mathbf{y}'']\exp(i\mathbf{y}''\cdot\mathbf{R}\mathbf{x})g[\mathbf{y}''], \tag{3.2b}$$

where $\mathbf{R}=\mathbf{R}[\mathbf{y}]$ and $\mathbf{y}''=\mathbf{R}\mathbf{y}'$, to obtain the right-hand side of the equation.

B. Wigner matrix

The action of the Wigner operator (3.1) on column vectors $\mathbf{f}\in\mathfrak{R}^{2l+1}$ [whose vector components are the observed wave field values (1.2)], is

$$\mathcal{W}(\mathbf{x})\mathbf{f}=\int_{\mathrm{SU}(2)} dg[\mathbf{y}]\exp(i\mathbf{x}\cdot\mathbf{y})\mathbf{D}^l[\mathbf{y}]\mathbf{f}=\mathbf{W}^l(\mathbf{x})\mathbf{f}, \tag{3.3}$$

where $\mathbf{D}^l[\mathbf{y}]$ are the spin-l unitary irreducible representation matrices of SU(2) in polar coordinates, well known as the *Wigner D-matrices* in angular momentum theory.[14,15] We call $\mathbf{W}^l(\mathbf{x})$ the SU(2) *Wigner W-matrices*; they are the *matrix representation* of the SU(2) Wigner operator on $\mathfrak{R}^{2l+1}$.

The Wigner *D*- and *W*-matrices are essentially Fourier conjugates of each other; the integral in Eq. (3.3) can be inverted because it has the transform kernel $\exp(i\mathbf{x}\cdot\mathbf{y})$. Thus, the transform pair is

$$\mathbf{W}^l(\mathbf{x})=\int_{\mathrm{SU}(2)} \gamma(|\mathbf{y}|)d\mathbf{y}\ \exp(i\mathbf{x}\cdot\mathbf{y})\mathbf{D}^l[\mathbf{y}], \tag{3.4a}$$

$$\mathbf{D}^l[\mathbf{y}]=\frac{1}{(2\pi^3)\gamma(|\mathbf{y}|)}\int_{\mathfrak{R}^3} d\mathbf{x}\ \exp(-i\mathbf{x}\cdot\mathbf{y})\mathbf{W}^l(\mathbf{x}). \tag{3.4b}$$

From (3.4) we see that since the Wigner *D*-matrices are unitary, $(\mathbf{D}^l[\mathbf{y}])^\dagger=\mathbf{D}^l[-\mathbf{y}]$, and since we have chosen the integration range to be invariant under inversions, it follows that $\mathbf{W}^l(\mathbf{x})^\dagger=\mathbf{W}^l(\mathbf{x})$, i.e., the Wigner *W*-matrices are self-adjoint. Therefore, their eigenvalues, determinant and trace, are real. Also from (3.4), the known integral and a special value of the *D*-matrices imply

$$\mathbf{W}^l(\mathbf{0})=\int_{\mathrm{SU}(2)} dg[\mathbf{y}]\mathbf{D}^l[\mathbf{y}]=2\pi^2\delta_{l,0}, \tag{3.5a}$$

$$\int_{\mathfrak{R}^3} d\mathbf{x}\mathbf{W}^l(\mathbf{x})=(2\pi)^3\gamma(\mathbf{0})\mathbf{D}^l[\mathbf{0}]=\pi^3\mathbf{1}. \tag{3.5b}$$

The unitarity of the *D*-matrices in (3.4a) further determines the integral

$$\int_{\mathfrak{R}^3} d\mathbf{x}[\mathbf{W}^l(\mathbf{x})]^\dagger\mathbf{W}^l(\mathbf{x})=(2\pi)^3\int_{\mathrm{SU}(2)}[\gamma(|\mathbf{y}|)]^2d\mathbf{y}\mathbf{1}=\pi^4 s_4\mathbf{1}, \tag{3.6}$$

where $s_4=\int_0^{2\pi}\mathrm{sinc}^4\ z\ dz=1.0467...$ is a constant. Finally, notice that (3.4) is a transform pair between functions W of $\mathbf{x}\in\mathfrak{R}^3$ and functions D of $g[\mathbf{y}]\in\mathrm{SU}(2)$ with support inside a sphere of radius 2π in $\mathfrak{R}^3$. Payley–Wiener theorems should yield analiticity properties of the Wigner *W*-matrices that will be explored elsewhere.

C. Wigner function and its covariance

We define the *Wigner distribution function* of the finite signals $\mathbf{f}=\{f_m\}_{m=-l}^{l}$ and $\mathbf{g}=\{g_m\}_{m=-l}^{l}$ as the sesquilinear form

$$W^l(\mathbf{f},\mathbf{g}|\mathbf{x}) = \mathbf{f}^\dagger \mathbf{W}^l(\mathbf{x})\mathbf{g} = \sum_{m,m'=-l}^{l} [f_m]^* W^l_{m,m'}(\mathbf{x}) g_{m'}. \tag{3.7}$$

The Wigner matrix elements are, from (2.7), (2.10), and (3.4a),

$$W^l_{m,m'}(\chi\mathbf{u}) = \int_{-2\pi}^{2\pi} \tfrac{1}{2}\sin^2\tfrac{1}{2}\eta d\eta \int_{\mathcal{S}_2} d\mathbf{v}\, \exp(i\chi\eta\mathbf{u}\cdot\mathbf{v}) D^l_{m,m'}[\eta\mathbf{v}]. \tag{3.8}$$

In Dirac's notation one can usefully write $W^l_{m,m'}(\mathbf{x}) = \langle l,m|\mathcal{W}(\mathbf{x})|l,m'\rangle$. When $\mathbf{f}=\mathbf{g}$, we indicate the Wigner function simply by $W^l(\mathbf{f}|\mathbf{x})$; this is the expectation value of the Wigner operator in the state $\mathbf{f}$.

From the SU(2)-covariance of the Wigner operator (3.2) follows the SU(2)-covariance of the Wigner matrix and of the Wigner function,

$$\mathbf{D}^l[\mathbf{y}]\mathbf{W}^l(\mathbf{x})\mathbf{D}^l[-\mathbf{y}] = \mathbf{W}^l(\mathbf{R}[\mathbf{y}]\mathbf{x}), \tag{3.9}$$

$$W^l(\mathbf{D}^l[-\mathbf{y}]\mathbf{f},\mathbf{D}^l[-\mathbf{y}]\mathbf{g}|\mathbf{x}) = W^l(\mathbf{f},\mathbf{g}|\mathbf{R}[\mathbf{y}]\mathbf{x}). \tag{3.10}$$

One consequence is that a signal vector $\boldsymbol{\alpha}^\mu = \{\alpha^\mu_m\}^l_{m=-l}$ which is an eigenvector of any operator $J_a = \mathbf{a}\cdot\mathbf{J}$ in the su(2) algebra and with the eigenvalue μ, will have a Wigner function that will be invariant under rotations of $\mathbf{x}$ around the axis $\mathbf{a}$. This is so because rotation by $\exp(-i\omega J_a)$ will multiply its eigenvector $\boldsymbol{\alpha}^\mu$ by $\exp(-i\omega\mu)$; but in (3.3)–(3.7) we see that the Wigner function is insensitive to common signal phase factors, $W^l(e^{i\phi}\mathbf{f}|\mathbf{x}) = W^l(\mathbf{f}|\mathbf{x})$. Such is the eigenbasis of *normal modes* of the finite wave guide, which are the eigenfunctions of the Hamiltonian H and given by the Kravchuk functions (2.5).

D. Meta-phase space

The definition, properties, and use of the common Wigner distribution function (1.1) were briefly discussed in the Introduction. We propose (3.7) as the proper Wigner function for finite signals $\mathbf{f}$ in a planar multimode wave guide. Equations (2.3)–(2.6) establish a correspondence between the (c-number) arguments of $W^l(\mathbf{f}|\mathbf{x})$ and the physical observables of a wave field in a shallow waveguide, namely,

$$\mathbf{x} = \chi\boldsymbol{\mu}(\vartheta,\varphi) = \begin{pmatrix} q \\ -p \\ E-l-\frac{1}{2} \end{pmatrix} = \begin{pmatrix} \text{position} \\ -\text{momentum} \\ \text{energy}-l-\frac{1}{2} \end{pmatrix}. \tag{3.11}$$

Because the first two coordinates are of ordinary phase space, let us call the three-dimensional space of $\mathbf{x}\in\mathfrak{R}^3$ the *metaphase space* of the finite wave guide model. When l is large and E is small, in a neighborhood of the South pole we can approximate the sphere $|\mathbf{x}|^2 = q^2+p^2+(e-l-\frac{1}{2})^2 \approx l^2$, by the osculating paraboloid $E \approx (p^2+q^2)/2l$, which corresponds to the classical energy in an oscillator. We should thus expect the values of the Wigner function to peak in $\chi = |\mathbf{x}|$ between l and $l+1$. This will be borne out below.

IV. WIGNER MATRIX AND PROJECTIONS

With the aim of computing the Wigner function of finite signals, we now find expressions for the D- and W-matrix elements and some of their main properties. To understand the results in three-dimensional space, we examine spherical slices and projections.

A. D^l matrix elements in polar coordinates

For analytic and computational work it is convenient to use both polar and Euler angle coordinate systems in SU(2). Their relation is

$$g[\mathbf{y}] = g(\phi,\theta,0)g(0,0,\eta)[g(\phi,\theta,0)]^{-1}, \quad \mathbf{y} = \eta\mathbf{v}(\theta,\phi), \tag{4.1}$$

where (θ,ϕ) determine the direction of the unit vector $\mathbf{v}$. This also holds for any matrix representation. The D-matrix elements are commonly written in terms of Euler angles as

$$D^l_{m,m'}(\phi,\theta,\psi)=e^{im\phi}d^l_{m,m'}(\theta)e^{im'\psi}, \tag{4.2}$$

where ϕ and ψ are rotations around the three-axis, $e^{im\phi}=\langle lm|e^{i\phi J_3}|lm\rangle$, and the *little-d*'s represent rotations around the one-axis, $d^l_{m,m'}(\theta)=\langle lm|e^{i\theta J_1}|lm'\rangle$, noting that we follow the convention of Vilenkin and Klymik[14] in rotating the second Euler angle around the one-axis; this is a form preferred for SO(N) systematics and is slightly different from that of Biedenharn and Louck in Ref. 15, Sec. 3.6, who rotate around the two-axis. The D-matrix elements in polar parametrization are thus bilinear in the d-functions,

$$\begin{aligned} D^l_{m,m'}[\eta\mathbf{v}(\theta,\phi)]&=\sum_{n=-l}^{l} D^l_{m,n}(\phi,\theta,0)e^{-in\eta}[D^l_{m',n}(\phi,\theta,0)]^* \\ &=e^{i(m'-m)\phi}\sum_{n=-l}^{l} d^l_{m,n}(\theta)e^{-in\eta}[d^l_{m',n}(\theta)]^*. \end{aligned} \tag{4.3}$$

B. W^l matrix elements on the two-sphere

Any point $\mathbf{x}=\chi\mathbf{u}(\vartheta,\varphi)\in\mathfrak{R}^3$ [cf. Eq. (2.7)] can be obtained by rotating $\chi\mathbf{k}=(0,0,\chi)$ from the North pole to $(\vartheta,\varphi)\in\mathcal{S}_2$, through

$$\mathbf{u}(\vartheta,\varphi)=\mathbf{R}(\varphi,\vartheta,0)\mathbf{k}. \tag{4.4}$$

Because of SU(2)-covariance (3.2a)–(3.9), we can write the Wigner W^l-matrix over the sphere in terms of its values at the North pole, where it is diagonal, $W^l_{m,m'}(\chi\mathbf{k})=\delta_{m,m'}W^l_m(\chi)$. Thus we have

$$W^l_{m,m'}(\chi\mathbf{u}(\vartheta,\varphi))=e^{-i(m-m')\varphi}\sum_{n=-l}^{l} d^l_{m,n}(\vartheta)W^l_n(\chi)[d^l_{m',n}(\vartheta)]^*, \tag{4.5}$$

which separates the angular dependence from the radial coordinate $\chi=|\mathbf{x}|\in\mathfrak{R}^+$, and

$$\begin{aligned} W^l_m(\chi)&=2\pi\sum_{n=-l}^{l}\int_{-1}^{1} d\,\cos\,\theta|d^l_{m,n}(\theta)|^2\int_{-2\pi}^{2\pi}\frac{1}{2}\sin^2\frac{1}{2}\,\psi d\psi\,\exp(i\psi[\chi\,\cos\,\theta-n]) \\ &=(-1)^{2l}\frac{\pi}{4}\sum_{n=-l}^{l}\int_{-1}^{1} ds|d^l_{m,n}(\arccos s)|^2 \\ &\quad\times\sin(2\pi\chi s)\left[\frac{-1}{\chi s-n+1}+\frac{2}{\chi s-n}+\frac{-1}{\chi s-n-1}\right], \end{aligned} \tag{4.6}$$

where in the last expression we have used $s:=\cos\,\theta$. Note that the integral we performed in ψ is the second difference in n of $\mathrm{sinc}\,2\pi(\chi s-n)$, and that the poles within the brackets cancel the zeros of the sine function. The eigenvalues of the self-adjoint Wigner matrix $\mathbf{W}^l(\chi\mathbf{u})$ are $\{W^l_m(\chi)\}^l_{m=-l}$. The Wigner matrix elements $W^l_{m,m'}(\mathbf{x})$ merit a deeper group-theoretical analysis; this will be done elsewhere, but it suffices to point out here that by virtue of their covariance properties, they are the *transform kernel* between functions of the continuous space coordinates $\mathbf{x}\in\mathfrak{R}^3$ and functions of the discrete space of irreducible representation indices (l,m,m'). They intertwine the angular momentum operators in their well-known differential form with their form (2.3) as difference operators.

C. Radial projection

The *radial marginal distribution* of the SU(2)-Wigner function $W^l(\mathbf{f},\mathbf{g}|\mathbf{x})$, $\mathbf{x}=\chi\mathbf{u}$, is its projection on the radius χ by integration over the spherical coordinates of $\mathbf{u}(\vartheta,\varphi)$,

$$M^l_{\text{radial}}(\mathbf{f},\mathbf{g}|\chi)=\int_{\mathcal{S}_2} d\mathbf{u}\,W^l(\mathbf{f},\mathbf{g}|\chi\mathbf{u}). \tag{4.7}$$

When we evaluate the integral (4.7) over $\mathbf{u}\in\mathcal{S}_2$, the exponential factor $\exp(i\chi\eta\mathbf{u}\cdot\mathbf{v})$ yields 4π sinc $\chi\eta$. Next, the $\mathcal{S}_2$-integral over the group parameters $\mathbf{v}(\theta,\phi)$ is computed by using

$$\int_{\mathcal{S}_2} d\mathbf{v}D^l_{m,m'}[\eta\mathbf{v}]=\frac{4\pi}{2l+1}\,\delta_{m,m'}\,\frac{\sin(l+\frac{1}{2})\eta}{\sin\frac{1}{2}\eta}. \tag{4.8}$$

Substituting, we obtain the radial projection of the Wigner function in the form

$$M^l_{\text{radial}}(\mathbf{f},\mathbf{g}|\chi)=(\mathbf{f},\mathbf{g})R^l(\chi), \tag{4.9}$$

where $(\mathbf{f},\mathbf{g})=\Sigma^l_{m=-l} f^*_m g_m$ is the inner product of the two signals (or the squared norm $|\mathbf{f}|^2$ of one signal when $\mathbf{f}=\mathbf{g}$). All radial dependence is contained in the factor

$$\begin{aligned}R^l(\chi)&=\frac{8\pi^2}{2l+1}\int_{-2\pi}^{2\pi} d\eta\,\sin\frac{1}{2}\,\eta\,\text{sinc}\,\chi\eta\,\sin\left(l+\frac{1}{2}\right)\eta\\&=\frac{4\pi^2}{(2l+1)\chi}\,[\text{Si}\,2\pi(\chi+l)+\text{Si}\,2\pi(\chi-l)-\text{Si}\,2\pi(\chi+l+1)-\text{Si}\,2\pi(\chi-l-1)],\end{aligned} \tag{4.10}$$

given in terms of the sine integral functions $\text{Si}\,x=\int_0^x \text{sinc}\,y\,dy$ (Ref. 16, Eq. 3.7632). Finally, the integral of the Wigner function over $\mathbf{x}\in\mathfrak{R}^3$ is proportional to the signal inner product (or squared norm),

$$M^l(\mathbf{f},\mathbf{g})=\int_{\mathfrak{R}^3} d\mathbf{x}W^l(\mathbf{f},\mathbf{g}|\mathbf{x})=\pi^3(\mathbf{f},\mathbf{g}). \tag{4.11}$$

In Fig. 2 we plot $R^l(\chi)$, the radial factor (4.10); taking into account (4.11) it shows that the Wigner function is concentrated in a spherical shell between radii $\chi=l$ and $l+1$. It is not difficult to show that the function $\chi R^l(\chi)$ has extremal points at every integer and half-integer $\chi\geqslant 0$, except for $\chi=l$ and $\chi=l+1$; the largest maximum of $\chi R^l(\chi)$ is at $\chi=l+\frac{1}{2}$, and $R^0(0)=2(2\pi)^3$. We emphasize that in $R^l(\chi)$ or $\chi^2R^l(\chi)$ (with the radial measure $\chi^2d\chi$), the position of this maximum shifts right or left (respectively) by small amounts but stays well within the interval $(l,l+1)$.

The number of sensors in the wave guide is fixed, so the Wigner function corresponds to a single value of l. In searching for convenient ways to plot this function of $\mathbf{x}\in\mathfrak{R}^3$, we have chosen to show its level curves on a *spherical slice* of $\mathfrak{R}^3$, for the standard value $\chi=l+\frac{1}{2}$. We have checked that similar plots at various radii near $l+\frac{1}{2}$ produce very similar figures, only with smaller maxima and curves somewhat more rounded. (Another graphing strategy for the Wigner function would be to project it by integration over χ with the radial measure $\chi^2d\chi$, or with any special or convenient measure; we leave this possibility open for future work.)

V. COHERENT STATES, ELEMENTARY STATES, CAT STATES

In this section we present the Wigner function of some signals of interest suggested by our group-theoretical treatment; they are concepts taken from the quantum theory of angular momentum. We direct our attention to coherent states and spherical harmonics.

A. Vacuum coherent state

The *vacuum* coherent state is the lowest-energy state (signal) of the system. For SU(2) and in the eigenbasis of J_3 it is the $(2l+1)$-dimensional column vector indicated

$$\boldsymbol{\alpha}(-\mathbf{k})=(0,\ldots,0,1)^{\mathsf{T}}, \tag{5.1}$$

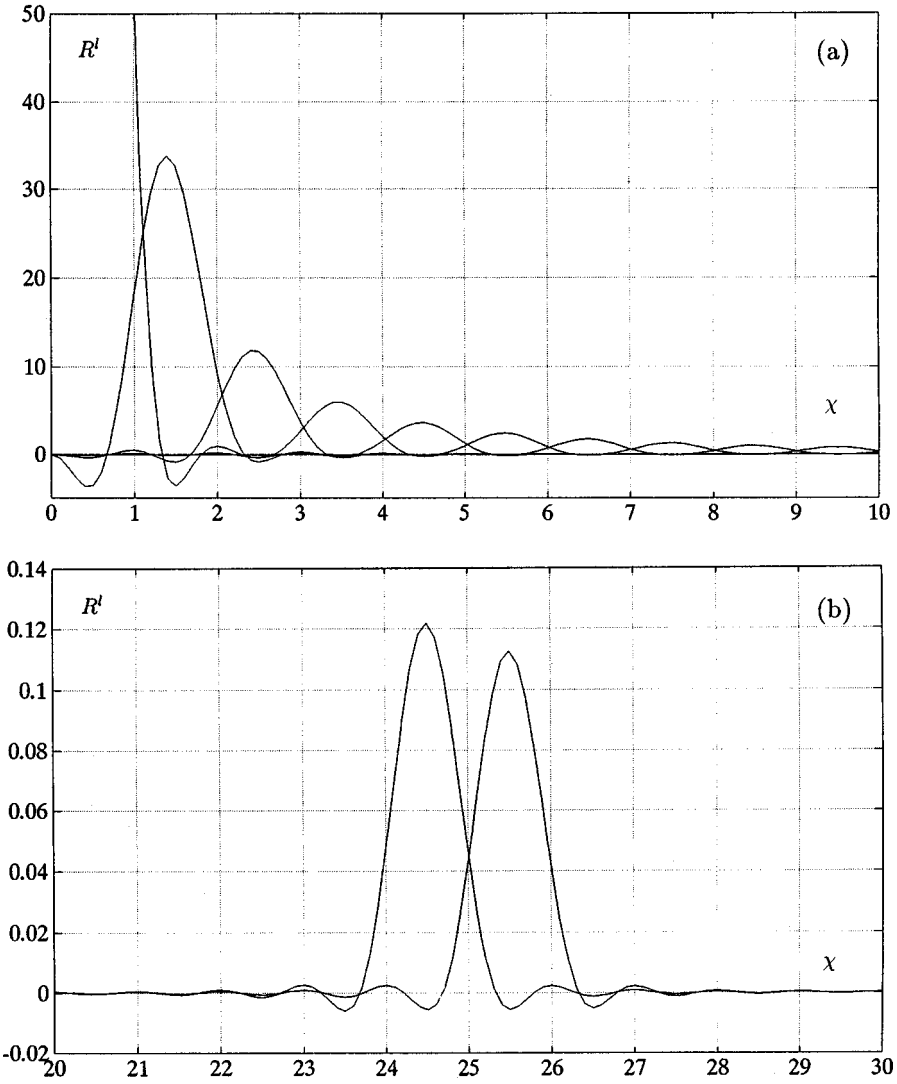

FIG. 2. Radial factor $R^l(\chi)$ in Eq. (4.10). (a) For $l=0,1,2,...,10$ in $0\leqslant\chi\leqslant 10$; the $l=0$ curve has its maximum value $2(2\pi)^3=496.10...$ at $\chi=0$. (b) Amplification of $l=24$ and $l=25$ in $20\leqslant\chi\leqslant 30$.

where T is the transpose and $-\mathbf{k}$ is a unit vector pointing to the South pole of the sphere.

In the basis where the position operator $Q=J_1$ is diagonal, the same state (5.1) represents the $(2l+1)$-point signal

$$\tilde{\boldsymbol{\alpha}}(-\mathbf{k})=\exp(-i\tfrac{1}{2}\pi J_2)\,\boldsymbol{\alpha}(-\mathbf{k})=\mathbf{D}^l(-\tfrac{1}{2}\pi,-\tfrac{1}{2}\pi,0)\,\boldsymbol{\alpha}(-\mathbf{k}), \tag{5.2a}$$

$$\tilde{\alpha}_m(-\mathbf{k})=e^{-i\pi m/2}d^l_{m,-l}(-\tfrac{1}{2}\pi)=\frac{e^{-i\pi m/2}}{2^l}\sqrt{\binom{2l}{l-m}}=e^{-i\pi m/2}\phi_0(m,2l). \tag{5.2b}$$

Here we recognize the Kravchuk function of order zero, $\phi_0(m,2l)$ in (2.5).[13] At the integers m, this function is the square root of the binomial distribution. In the limit when $l\to\infty$, $\phi_0(q,2l)$ becomes the Gaussian function of lowest oscillator state of quantum mechanics. In Fig. 3, the Wigner function (3.7) of the signal (5.2) is plotted on the sphere of radius $|\mathbf{x}|=l+\frac{1}{2}$,

$$W^l_{\text{sphere}}(\boldsymbol{\alpha}(-\mathbf{k}))|\,\vartheta,\varphi)=W^l_{-l,-l}(\chi\mathbf{u}(\vartheta,\varphi))\big|_{\chi=l+1/2}=\sum_{m=-l}^{l}W^l_m[d^l_{-l,m}(\vartheta)]^2, \tag{5.3}$$

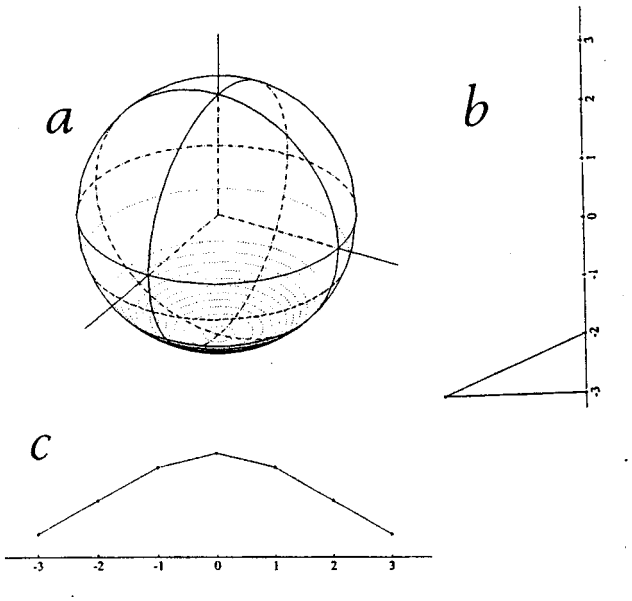

FIG. 3. Faces of the vacuum coherent state $\boldsymbol{\alpha}(-\mathbf{k})$ for $l=3$ and 7 ''sensor'' points: (a) Wigner function (5.3). Positive level contours are indicated with unbroken lines for function values 0.35, 0.7,...; zero and negative levels are indicated with broken lines. (b) Energy (mode) content. (c) The signal in the ''position'' ($Q=J_1$) basis of sensors; it is a Kravchuk function of order zero which is also the root of the binomial distribution.

where $W_m^l = W_m^l(l+\frac{1}{2})$ are constants obtained from (4.6) for the chosen value of the radius χ. Figure 3 shows the signal, its mode (energy) content, and the level curves of the Wigner function on the sphere; it shows the *partitura* of the vacuum coherent state, the ''fundamental note'' of the system. Evolution along the z-axis of the wave guide is generated by the Hamiltonian H in (2.3c), and appears as a rotation of the Wigner function around the three-axis of the sphere. Under this transformation, the vacuum state is simply multiplied by the phase $e^{-iz/2}$; hence its Wigner function is invariant.

B. SU(2) coherent states

The Wigner function of the vacuum coherent state can be rotated to any new position on the sphere (ϑ,φ) by means of SU(2)-optical transformations of the signal, i.e., by free propagation along a waveguide, with refracting wedges and tilted plates. One thus generalizes the concept of coherent states to $\boldsymbol{\alpha}(\mathbf{a})$ for any and all directions $\mathbf{a}(\vartheta,\varphi)\in\mathcal{S}_2$. If

$$\mathbf{a}=e^{i\vartheta J_1}e^{i\varphi J_3}\mathbf{k}, \quad \text{then} \quad \alpha_m(\mathbf{a}(\vartheta,\varphi))=D^l_{m,-l}(-\varphi,-\vartheta,0)=e^{im\varphi}d^l_{-l,m}(\vartheta) \tag{5.4}$$

are the components of the coherent state along **a**. In Figs. 4 we show the *antivacuum coherent* state $\boldsymbol{\alpha}(\mathbf{k})$, which is the highest energy mode in the finite planar wave guide. This is obtained from the vacuum state $\boldsymbol{\alpha}(-\mathbf{k})$ by a rotation of the sphere around the one-axis; such rotation can be physically produced with a refracting wedge that impresses a phase $e^{i\pi m}=(-1)^m$ on the input signal values; the output signal for continuous q is the Kravchuk function $\phi_{2l}(q,2l)$. For integer values m of q, this signal has the envelope of the vacuum coherent state $\phi_0(m,2l)$, but with values alternating in sign.

C. Elementary states

When the unit vector **a** is along the one-axis **i**, the coherent state $\boldsymbol{\alpha}(\mathbf{i})$ is the signal (1,0,...,0). When this signal propagates along the wave guide, the vector **a** will move around the equator; the signal will undergo the fractional Fourier–Kravchuk transformation cycle.[6] We call *elementary*

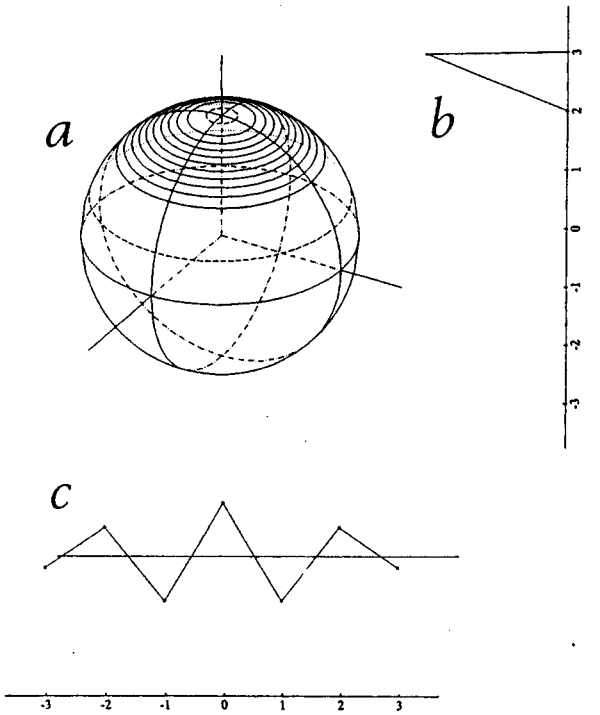

FIG. 4. Antivacuum coherent state $\boldsymbol{\alpha}(\mathbf{k})$ for $l=3$, with the parameters of the previous figure. (a) Wigner function. (b) Energy (mode) content. (c) Signal at the sensors ($Q=J_1$ basis) as in the previous figure but with alternating signs.

states (in an array of $2l+1$ sensors) to those signals with single 1 at some position ν ($l-\nu$ integer) and zeros on the rest. They are the eigenfunctions of J_1 with eigenvalues $\nu \in \{l, l-1, ..., -l\}$ and will be indicated by $\boldsymbol{\alpha}^{\nu}(\mathbf{i})$.

The Wigner function (3.7) of elementary states can be then written in polar coordinates $\mathbf{u}_1(\vartheta_1, \varphi_1)$, referred to the one-axis [so $\mathbf{u}_1(0, \varphi_1) = \mathbf{i}$],

$$W^l_{\text{sphere}}(\boldsymbol{\alpha}^{\nu}(\mathbf{i}) | \vartheta_1, \varphi_1) = W^l_{\nu,\nu}(\chi \mathbf{u}_1(\vartheta_1, \varphi_1))|_{\chi = l+1/2} = \sum_{m=-l}^{l} W^l_m [d^l_{\nu,m}(\vartheta_1)]^2. \tag{5.5}$$

[cf. Eq. (5.3).] The Wigner functions of elementary signals are independent of φ_1, and thus invariant under rotations of the sphere around the one-axis. Conversely, when the Wigner function of a signal $\mathbf{f}$ is invariant under rotations around some axis $\mathbf{a}$, $\mathbf{f}$ can be multiplied only by an overall phase when acted upon by $\exp(i\omega \mathbf{a}\cdot\mathbf{J})$; therefore $\mathbf{f}$ will be an eigenfunction of $\mathbf{a}\cdot\mathbf{J}$. From the plot of the Wigner function one can determine readily whether or not an output signal $\mathbf{f} = \{f_m\}^l_{m=-l}$ derives from the input of an elementary signal (0,...,0,1,0,...,0) through an SU(2)-optical system.

D. Schrödinger-cat signals and their smile function

The sum of two signals is a *Schrödinger-cat signal*. The original Schrödinger ''paradox'' of coherently superposing one dead and one live cat states applies fruitfully to signal analysis.

Consider two signals $\mathbf{f}$ and $\mathbf{g}$; the Wigner function of their linear combination $c_f\mathbf{f} + c_g\mathbf{g}$ is

$$W(c_f\mathbf{f} + c_g\mathbf{g} | \mathbf{x}) = |c_f|^2 W(\mathbf{f}|\mathbf{x}) + |c_g|^2 W(\mathbf{g}|\mathbf{x}) + 2\,\text{Re}\, c_f^* c_g W(\mathbf{f},\mathbf{g}|\mathbf{x}). \tag{5.6}$$

The Wigner functions of the two signals thus not only add, but *interfere*. The cross term $S(\mathbf{f},\mathbf{g}|\mathbf{x}) = 2\,\text{Re}\,\mathbf{f}^\dagger \mathbf{W}(\mathbf{x})\mathbf{g}$ has been called the *smile* function of the Schrödinger-cat state; it is a most prominent feature of the Wigner function of cat states that carries the holographic information of the object signal $\mathbf{g}$ with the reference signal $\mathbf{f}$.[17]

In Fig. 5 we plot Schrödinger cat states composed of two normal modes of the wave guide, for $l=3$ and 7 sensors. If we place the one-axis along the three-axes of the figures, the Schrödinger

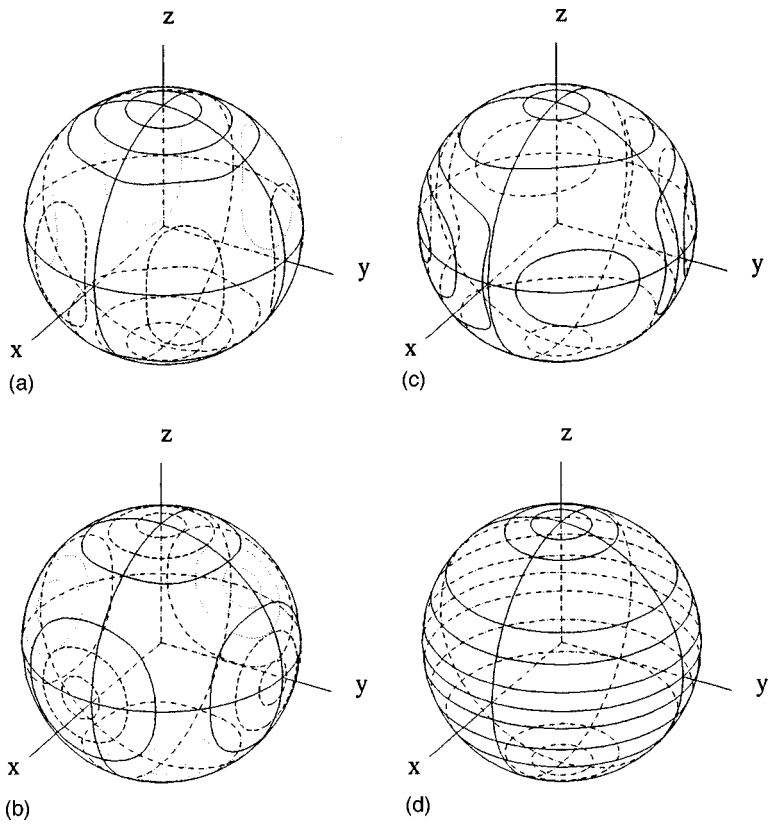

FIG. 5. Schrödinger-cat states of two normal modes or elementary seven-point signals ($l=3$). (a) ($1/\sqrt{2}$, 0, 0, 0, 0, 0, $1/\sqrt{2}$), (b) (0, $1/\sqrt{2}$, 0, 0, 0, $1/\sqrt{2}$, 0), (c) (0, 0, $1/\sqrt{2}$, 0, $1/\sqrt{2}$, 0, 0), and (d) (0,0,0,1,0,0,0).

cats are ''bilocalized'' states and the last is an elementary state. Compare Fig. 5(a) with Figs. 3 and 4, noticing the six oscillations (*teeth*) of the smile across the equator; Fig. 5(b) exhibits four, Fig. 5(c) shows two, and Fig. 5(d) has axial symmetry.

VI. CONCLUDING REMARKS

We represented finite data sets by their Wigner function in an optical model of planar multimodal wave guides. Position, momentum, and energy (mode number) are *c*-number coordinates which are associated to the generators of su(2) algebra; the latter are self-adjoint difference operators with discrete, equally-spaced, and finite spectra. The *partitura* of a signal is drawn on a sphere. The vacuum coherent state is analogous to the ground harmonic oscillator wave function; from it, all other coherent states can be produced by SU(2)-optical elements, wave guide, wedge, and slab. These transformations are the counterpart of rotation and translation of classical phase space.

The applicability of our construction extends to other mechanical and optical systems, also based on finite data sets but with different dynamics. For instance, the quantum *point rotor* (a mass point constrained to move on $\mathcal{S}_2$) has symmetry group SO(3), which is covered twice by SU(2). This system is isomorphic to the mechanical vibrating sphere and, by stereographic projection, to the two-dimensional Maxwell fisheye wave-optical medium.[18] In both of these cases, wave functions are on the sphere and generally contain *all* spherical harmonics,

$$\Psi(\beta,\gamma)=\sum_{l=0}^{\infty}\sum_{m=-l}^{l}\Psi_m^l Y_m^l(\beta,\gamma). \tag{6.1}$$

The data set is now infinite and given by the tower of coefficients $\mathbf{\Psi}=\{\mathbf{\Psi}^l\}_{l=0}^{\infty}$, $\mathbf{\Psi}^l=\{\Psi_m^l\}_{m=-l}^{l}$.

The SU(2) Wigner function (3.7) was built for a single value of l corresponding to a fixed number of sensors of the model, and the radial factor (4.10) indicated that it is concentrated in a spherical shell of mean radius $l+\frac{1}{2}$. If now the data vector is (6.1), the Wigner operator (3.1) will act irreducibly on each subvector $\mathbf{\Psi}^l$, and the Wigner function of $\mathbf{\Psi}$ will be the sum of the Wigner functions in the irreducible subspaces, i.e.,

$$W(\mathbf{\Psi}|\mathbf{x})=\sum_{l=0}^{\infty} W^l(\mathbf{\Psi}^l|\mathbf{x})=\sum_{l=0}^{\infty} \mathbf{\Psi}^{l\dagger}\mathbf{W}^l(\mathbf{x})\mathbf{\Psi}^l. \tag{6.2}$$

Such a function must be plotted in $\mathfrak{R}^3$-space $\mathbf{x}$ and will show the quasiprobability distribution of the angular momentum vector $\mathbf{J}$ in the mechanical model, and of the beam parameters in the Maxwell fisheye. As drawn in elementary texts, the extreme spherical harmonic (coherent state) $Y_l^l(\beta,\gamma)$ has a minimal uncertainty cone around the three-axis, $Y_{l-1}^l(\beta,\gamma)$ has a larger cone, etc., until $Y_0^l(\beta,\gamma)$ opens the cone into the equator. Thus, while the wave function on the sphere $Y_l^l(\beta,\gamma)$ have their square maximum on the equator $\beta=\frac{1}{2}\pi$ (where the classical particle is), the Wigner function is concentrated in the North polar cap around $\mathbf{x}=(l+\frac{1}{2})\mathbf{k}$ (where the angular momentum is). On the other hand, strongly localized rotor wave functions, containing a wide spread of l's, will have Wigner functions (6.2) widely spread in $|\mathbf{x}|$.

The dynamics of the rotor models (vibrating sphere and Maxwell fisheye) are different from the wave guide, however; their Hamiltonian is proportional to the Casimir operator of so(3)=su(2), rather than to one of its generators. Since under the corresponding ''time'' evolution τ, each component $\mathbf{\Psi}^l$ is multiplied by the phase $\exp[i\tau l(l+1)]$, it follows that the Wigner function (6.2) is invariant under rotor dynamics.

Nonlinear processes on discrete, finite systems, can also be analyzed with the SU(2) Wigner function (3.7) when the Hamiltonian belongs to the su(2) *enveloping* algebra. This is the case of the finite analog of the optical Kerr medium studied in Ref. 19, whose Hamiltonian is $\sim J_3+\alpha J_3^2$. It also applies for Hamiltonians contrieved to have the form $\frac{1}{2}J_2^2+V(J_1)$, to mimic the classical form of mechanics $\frac{1}{2}p^2+V(q)$, but restricted to a finite number of bound states. Natural applications for SU(2)-Wigner functions will also include spin and pseudo-spin systems, as they appear, e.g., in quantum optics, when a collection of two-level atoms interact with the radiation field under small-volume approximation, as in the Dicke model.[20,21] Time evolution in these cases deforms the shape of the initial coherent state on the sphere; in the Kerr medium, the SU(2) Wigner function gives a transparent picture of the nature of fractional-period resonances.[19] Covariance does not hold beyond SU(2), so we can expect purely quantum effects (including squeezing) to show up in the Wigner function on the sphere.

ACKNOWLEDGMENTS

We are very grateful to the referee for carefully reading the original manuscript and his critical remarks which have helped us greatly to improve the presentation of our results. We thank Guillermo Krötzsch for his kind help with the figures. This work was performed under the support of Project DGAPA-UNAM 106595 *Optica Matemática.*

[1] E. Wigner, ''On the quantum correction for thermodynamic equilibrium,'' Phys. Rev. **40**, 749–759 (1932); M. Hillery, R. F. O'Connell, M. O. Scully, and E. P. Wigner, ''Distribution functions in physics: Fundamentals,'' Phys. Rep. **106**, 121–167 (1984); H.-W. Lee, ''Theory and application of the quantum phase-space distribution functions,'' *ibid.* **259**, 147–211 (1995).

[2] A. Lohmann, ''The Wigner function and its optical production,'' Opt. Commun. **42**, 32–37 (1980).

[3] H. O. Bartelt, K.-H. Brenner, and H. Lohmann, ''The Wigner distribution function and its optical production,'' Opt. Commun. **32**, 32–38 (1980); H. Bartelt and K.-H. Brenner, ''The Wigner distribution function: An alternate signal representation in optics,'' Isr. J. Tech. **18**, 260–262 (1980); K.-H. Brenner and H. Lohmann, ''Wigner distribution function display of complex 1D signals,'' Opt. Commun. **42**, 310–314 (1982).

[4] G. Gasper and M. Rahman, *Basic Hypergeometric Series* (Cambridge University Press, Cambridge, 1990); A. F. Nikiforov, S. K. Suslov, and V. B. Uvarov, *Classical Orthogonal Polynomials of a Discrete Variable* (Springer, Berlin, 1991).

[5] K. B. Wolf, *Integral Transforms in Science and Engineering* (Plenum, New York, 1979), Chap. 1–3.

[6] N. M. Atakishiyev and K. B. Wolf, ''Fractional Fourier–Kravchuk transform,'' J. Opt. Soc. Am. A **14**, 1467–1477 (1997).

[7] K. B. Wolf, ''Wigner distribution function for paraxial polychromatic optics,'' Opt. Commun. **132**, 343–352 (1996).

[8] J. W. Goodman, *Introduction to Fourier Optics* (McGraw–Hill, New York, 1968).

[9] J. R. Klauder and E. C. G. Sudarshan, *Fundamentals of Quantum Optics* (Benjamin, Reading, 1968).

[10] L. M. Nieto, N. M. Atakishiyev, S. M. Chumakov, and K. B. Wolf, ''Wigner distribution function for Euclidean systems,'' J. Phys. A **31**, 3875–3895 (1998).
[11] N. M. Atakishiyev and S. K. Suslov, ''Difference analogs of the harmonic oscillator,'' Theor. Math. Phys. **85**, 1055–1062 (1991).
[12] M. Krawtchouk, ''Sur une généralization des polinômes d'Hermite,'' C. R. Acad. Sci., Paris **189**, 620–622 (1929); A. Erdélyi, W. Magnus, F. Oberhettinger, and F. G. Tricomi, *Higher Transcendental Functions* (McGraw–Hill, New York, 1953), Vol. 2.
[13] N. M. Atakishiyev and K. B. Wolf, ''Approximation on a finite set of points through Kravchuk functions,'' Rev. Mex. Fis. **40**, 366–377 (1994).
[14] N. Ja. Vilenkin and A. U. Klimyk, *Representation of Lie Group and Special Functions* (Kluwer Academic, Dordrecht, 1991), Vol. 1.
[15] L. C. Biedenharn and J. D. Louck, *Angular Momentum in Quantum Physics*, in the Encyclopedia of Mathematics and its Applications Series, edited by G.-C. Rota (Addison–Wesley, Reading, 1981).
[16] I. S. Gradshteyn and I. M. Ryzhik, *Table of Integrals, Series, and Products*, 4th ed. (Academic, New York, 1965).
[17] K. B. Wolf and A. L. Rivera, ''Holographic information in the Wigner function,'' Opt. Commun. **144**, 36–42 (1997).
[18] A. Frank, F. Leyvraz, and K. B. Wolf, ''Hidden symmetry and potential group of the Maxwell fish-eye,'' J. Math. Phys. **31**, 2757–2768 (1990).
[19] S. M. Chumakov, A. Frank, and K. B. Wolf, ''Finite Kerr medium: Schrödinger cats and Wigner functions on the sphere'' (preprint No. 65, IIMAS-UNAM, October 1997) (submitted).
[20] R. H. Dicke, ''Coherence in spontaneous radiation processes,'' Phys. Rev. **93**, 99–110 (1954); D. J. Wineland, J. J. Bollinger, W. M. Itano, and D. J. Heinzen, ''Squeezed atomic states and projection noise in spectroscopy,'' Phys. Rev. A **50**, 67–88 (1994).
[21] M. Kozierowski, A. A. Mamedov, and S. M. Chumakov, ''Spontaneous emission by a system of N two-level atoms in terms of the SU(2)-group representations,'' Phys. Rev. A **42**, 1762–1766 (1990); S. M. Chumakov and M. Kozierowski, ''Collective emission in a lossless cavity: Analytical approach,'' Quantum Semiclassic. Opt. **8**, 775–803 (1996).